Complex Signal Processing is Not Complex

Kenneth W. Martin, *Fellow, IEEE*

Abstract—**Wireless systems often make use of the quadrature relationship between pairs of signals to effectively cancel out-of-band and interfering in-band signal components. The understanding of these systems is often simplified by considering both the signals and system transfer functions as *"complex"* quantities. The complex approach is especially useful in highly integrated multistandard receivers where the use of narrow-band fixed-coefficient filters at the RF and high IF must be minimized. This paper first presents a tutorial review of complex signal processing for wireless applications. The review emphasizes a graphical and pictorial description rather than an equation-based approach. Next, a number of classical modulation architectures are described using this formulation. Finally, more recent developments such as complex filters, image-reject mixers, low-IF receivers, and oversampling analog–digital converters are discussed.**

Index Terms—**Communication systems, complex signal processing, filters, frequency modulation, mixers, wireless receivers.**

I. INTRODUCTION

THIS paper is intended to be used as a tutorial introduction to complex signal processing, and also as an illustration of its wide use in a number of different applications, both analog and digital, in recent communication systems.

A *complex* signal consists of a pair of *real* signals at an instant in time. If one denotes the complex signal $X(t)$, as $X(t) = x_r(t) + jx_q(t)$ where $j = \sqrt{-1}$; then, a Hilbert space can be defined using appropriate definitions for addition, multiplication, and an inner product and norm. In an actual physical system, the signals are both real (but are called the real and imaginary parts) and are found in two distinct signal paths. The multiplier "j" is used to help define operations between different complex signals, and is to some degree *imaginary*; i.e., it does not actually exist in actual systems. Often, the dependence of signals on time is not shown explicitly.

The use of *complex* signal processing to describe wireless systems is increasingly important and ubiquitous for the following reasons: it often allows for image-reject architectures to be described more compactly and simply; it leads to a graphical or signal-flow graph (SFG) description of signal-processing systems providing insight, and it often leads to the development of new systems where the use of high-frequency highly selective image-reject filters is minimized. The result is more highly integrated systems using less power and requiring less physical space.
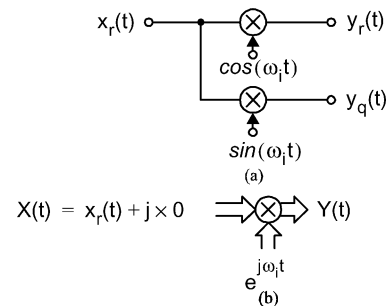
Fig. 1. SFG of an quadrature mixer using (a) a real SFG and (b) a complex SFG.

As an example, consider the popular "*quadrature*" mixer with a *real* input as shown in Fig. 1. In the complex SFG, two real multiplications have been replaced by a single complex multiplication. Furthermore, since in the time domain, we have

$$Y(t) = y_r(t) + jy_q(t)$$
$$= X(t)e^{j\omega_i t} \tag{1}$$

then, taking the Fourier transform, we have

$$Y(\omega) = X(\omega - \omega_i) \tag{2}$$

and we see that an ideal quadrature mixer results in a simple frequency shift of the input signal with no images occurring, a conclusion that is obvious from Fig. 1(b), but is certainly not obvious from Fig. 1(a). If this mixer is followed by a low-pass filter in each path, then, it can be used to directly demodulate carrier-frequency signals without images as is discussed in Section III-A. For this reason, it often called an *image-reject mixer* although if one is being accurate, the term should denote the combination of the quadrature mixer and low-pass filters.

The use of complex signal processing for wireless applications has blossomed recently. This is especially true for high-bit-rate standards, such as local-area networks (LANs), and for multistandard transceivers. Evidence of this proliferation is that in 2001, 2002, and 2003, the *majority* of the papers in *IEEE International Solid-State Circuits Conference* sessions on wireless transceivers for LAN applications employed complex signal processing.

Much, but not all of this paper deals with the already mentioned tutorial review of complex signal processing, especially as it is applicable to wireless systems. A great deal of the tutorial material on complex *analog* signal processing is directly based on the research of Snelgrove, as described in [1], [6], [7], and in some theses by his graduate students [9], [11]. Unfortunately, a journal submission describing this early work was rejected, but a reprint of the originally submitted paper can be obtained from [8]. Some of the early published work on complex *digital* filters is described in [2] and [5].

In the course of the review of the fundamentals of complex signal processing, some important identities are given. Examples are given using complex SFG representations. In Section III, a number of classical wireless modulations systems are described using the complex formulation. These systems include Weaver and Hartley modulators and polyphase filters. Errors due to nonideal coefficients in mixers are quantified. In Section IV, complex analog and digital filters are discussed. Section III describes more-recent complex signal-processing applications. These include, for example, complex adaptive image-reject mixers, and complex low-IF receiver architectures including a new modulation approach that doubles the data rate for a given analog–digital (A/D) sampling frequency, and complex bandpass oversampling A/D converters. These systems are especially useful in multistandard wireless applications as they are inherently wide-band (without excessive imaging errors) and allow the systems to be adapted to individual standards using digital programming after the A/D converters.

II. COMPLEX SIGNAL PROCESSING

Complex signal processing systems operate on ordered pairs of real signals. A possible definition for a complex inner product is

$$\langle x_1(t), x_2(t) \rangle = \lim_{t \to \infty} \frac{1}{2t} \int_{-t}^{t} x_1(\tau) x^*_2(\tau) d\tau. \qquad (3)$$

Combining this definition with the typical definitions for complex inversion, addition, and multiplication, and with the properties of commutation and association, constitutes a Hilbert space. It is assumed that all signals are periodic and frequency limited, and therefore, can be expressed as a finite series of "*complexoids*"[1]

$$x_i(t) = \sum_{i=-N}^{N} k_i e^{j\omega_0 i t} \qquad (4)$$

where k_i is, in general, complex [5]. In this paper, we will limit our consideration normally to a single (or a few) complexoids in order to simplify explanations.

A. Complex Operations

Most complex systems are realized using only four basic operations: complex addition, complex multiplication, and complex integration for continuous-time filters or complex delay for discrete time filters. In addition, the operation of complex conjugation is required to describe imaging errors due to mismatch and quadrature imbalance in real physical systems.

A complex addition of two complex signals simply adds the two real parts and the two imaginary parts independently. Consider the real SFG that represents adding a complex signal to a second complex signal, as is shown in Fig. 2(a). Its complex SFG is shown in Fig. 2(b).
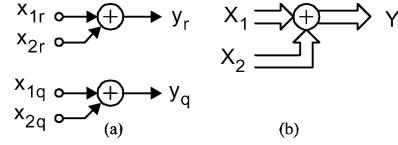

Fig. 2.   (a) Real SFG for adding two complex signals. (b) Equivalent complex SFG.
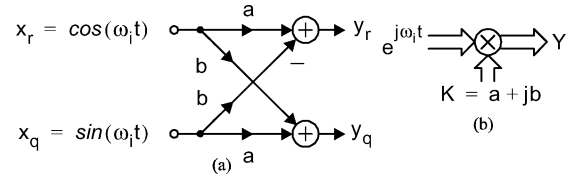

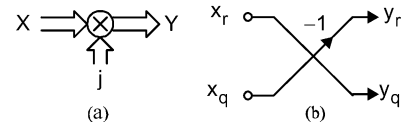Fig. 3.   (a) Real SFG of a complex multiplication. (b) Equivalent complex SFG.

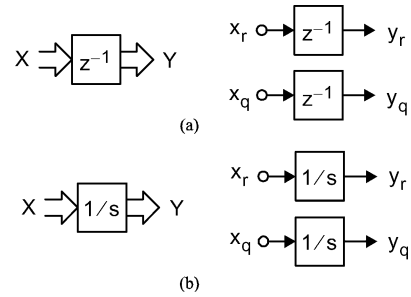Fig. 4.   Multiplying a signal by the imaginary constant j.

Fig. 5.   (a) Digital delay operator. (b) Analog integration operator for complex signals.

Slightly more complicated is a complex multiplication; consider multiplying a complexoid $X(t) = e^{j\omega_i t}$ by a complex coefficient $K = a + jb$. We have

$$Y(t) = \{a\cos(\omega_i t) - b\sin(\omega_i t)\} \\ + j\{a\sin(\omega_i t) + b\cos(\omega_i t)\}. \qquad (5)$$

The real SFG of this operation is shown in Fig. 3(a). Once again the complex SFG of a multiplication operation, as shown in Fig. 3(b), is considerably simpler. Note that the real SFG does not include the constant j anywhere, whereas, in the complex SFG, it is admissible.

A special case is the multiplication of an input signal by the constant j. This is shown using Fig. 4(a) and a real SFG in Fig. 4(b). This operation is simply an interchanging of the real and inverted imaginary parts; this operation is the basis of realizing imaginary components in complex networks; that is, imaginary gains are realized by cross coupling in the two real networks.

Two additional operations are required for realizing complex filters, namely, the delay operator for digital filters and the integration operator for analog filters. These operations simply consist of independently applying the corresponding real operation to each part of the complex signal, as shown in Fig. 5.

---

[1]The author has taken the liberty of coining the word "*complexoid*" to represent the complex single-frequency signal component $e^{j\omega t} = \cos(\omega t) + j\sin(\omega t)$
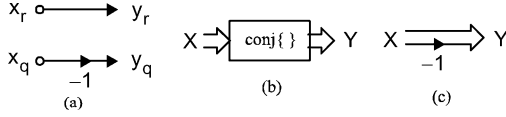
Fig. 6. Complex conjugation operation.

Another operation, which is important for quantifying imaging caused by component mismatch errors, is complex conjugation. Consider

$$X(t) = Me^{j\phi}e^{j\omega_i t} \tag{6}$$

with M real. We have

$$X^*(t) = Me^{-j\phi}e^{-j\omega_i t} \tag{7}$$

and we see that besides being phase rotated, X has been transformed from a positive-frequency complexoid into a negative-frequency complexoid. Conjugation also changes negative-frequencies complexoids to positive frequencies. The conjugation operation is shown in the real SFG of Fig. 6(a). Alternative complex SFGs are shown in Fig. 6(b) and (c).

B. Rectangular to Polar Duality

Consider two parallel real systems having components at a single frequency ω_i in each path, where the signals do not have quadrature balance; that is, the amplitudes do not match, and the phases are not different by exactly $\pm 90°$. In this general case, assuming the signals in the second path are always to be multiplied by j, we can express the signal $X(t)$ in rectangular form as

$$X(t) = A\cos(\omega_1 t + \phi_1) + jB\sin(\omega_1 t + \phi_2). \tag{8}$$

If the signals had quadrature balance, then, we would have $A = B$ and $\phi_1 = \phi_2$; in the quadrature-imbalanced case, this is not true. Using simple trigometric identities, it is straightforward to show $X(t)$ can equivalently be expressed in polar form as

$$X(t) = Pe^{j\omega_i t} + Ne^{-j\omega_i t} \tag{9}$$

where P and N are possibly complex coefficients and given by

$$P = \frac{Ae^{j\phi_1} + Be^{j\phi_2}}{2} \tag{10}$$

and

$$N = \frac{Ae^{-j\phi_1} - Be^{j\phi_2}}{2}. \tag{11}$$

Thus, quadrature-imbalanced signals, at a single frequency, can be expressed as two complexoids, one at positive frequencies, and one at negative frequencies.

Alternatively, given a positive and negative complexoid at a single frequency expressed as in (9), one can equivalently represent them in the rectangular form of (8) where

$$A = |P + N^*|, \ \phi_1 = \angle(P + N^*) \tag{12}$$

and

$$B = |P - N^*|, \ \phi_2 = \angle(P - N^*). \tag{13}$$

This important duality, along with some simple trigometric identities, is useful in quantifying many of the imaging nonidealities of communication systems, as we shall see later.

C. Hilbert Transforms and Positive-Pass Filters

An important example of a complex signal processing system is that of a *positive-pass filter* (PPF) (or alternatively that of a *negative-pass filter* or NPF). This is a filter that can take a possibly complex but quadrature-imbalanced input signal[2] and produce a necessarily complex quadrature-balanced output signal that has positive frequency components only. A signal with positive-frequency components only is called an *analytic signal*. It has the property that, for every real spectral component, there is a corresponding imaginary spectral component that is equal in magnitude but *delayed in time* by 90°[1]. A complex SFG of a system that produces analytic signals from possibly complex signals is shown in Fig. 7(a), and the equivalent real SFG is shown in Fig. 7(b). As shown, Hilbert transform filters are required to produce the signals delayed in time by 90°. For negative frequencies, which have phases continually changing to more negative values, this means the outputs are phase shifted by +90°, as opposed to −90° for positive frequencies, which have phases that increase in time.[3] Consider the system in Fig. 7 for a positive frequency input of $X = e^{j\omega_i t}$. We have

$$Y = \frac{1}{2}[X + j(-j)X] = e^{j\omega_i t} \tag{14}$$

and the input signal is unchanged. However, for a negative frequency input of $X = e^{-j\omega_i t}$, we have

$$Y = \frac{1}{2}[X + j(j)X] = 0. \tag{15}$$

The PPF of Fig. 7, which is based on using the Hilbert transform, can be considered a particular case of a complex filter. The concept of a PPF (or an NPF) can be generalized to that of complex filters which have passbands at positive frequencies only (or negative frequencies only). Complex filters are discussed in Section IV.

III. COMPLEX MODULATION AND CLASSICAL WIRELESS SYSTEMS

We have seen in the Introduction that a real input signal can be frequency shifted without imaging errors, using two real multipliers as shown in Fig. 1. This operation ideally shifts both positive and negative frequency components in the same direction by the same amount. This operation, when combined with an appropriate low-pass filter, can be used to frequency demodulate an RF input to a complex IF frequency or directly to baseband [12]–[14].

---

[2]Most texts [5] only consider the special case of real input signals.

[3]This is inherent in the conjugate-symmetry property of real transfer functions.
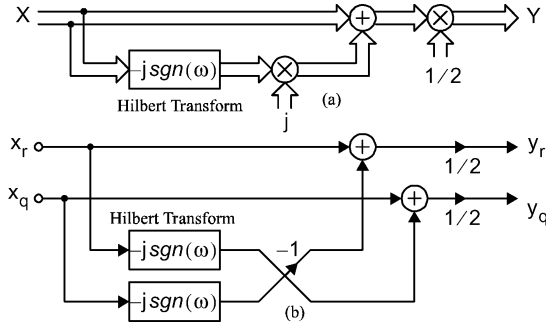
Fig. 7. One possibility for realizing a PPF: (a) a complex SFG, and (b) an equivalent real SFG.
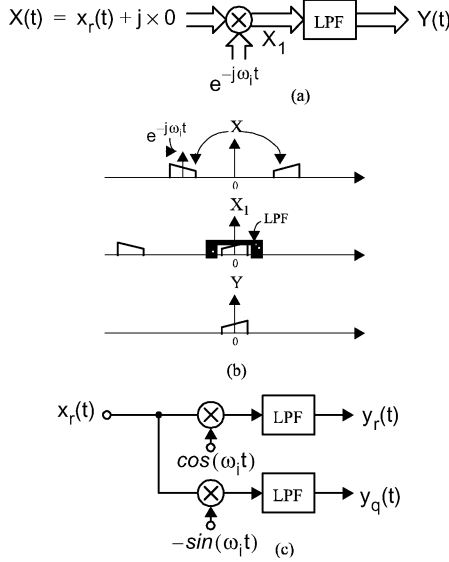

Fig. 8. Image-reject down converter. (a) Complex SFG. (b) Example spectra. (c) Equivalent real SFG.

A. Direct-Conversion Receiver

The direct-conversion receiver is a good choice of architecture for less demanding but highly integrated applications [43], [44]. A simplified receiver architecture, using both a complex SFG (and a real SFG), is shown in Fig. 8. Example spectra of various locations of Fig. 8(a) are shown in Fig. 8(b).

B. Direct-Conversion Transmitter

In a direct-conversion transmitter, a complex input signal is directly modulated to RF using a complex mixer, and then converted to a real RF signal by simply ignoring the imaginary output of the complex mixer; this process allows us to simplify the complex mixer to two real multipliers, as is shown in Fig. 9(c).

C. Single-Sideband (SSB) Generation

One of the first uses of complex processing in wireless systems was for SSB generation. For example, consider the Weaver architecture, as is shown in Fig. 10.[4] In this approach, the baseband signal, which is symmetric about dc, is frequency shifted

---

[4]This is a good example of how complex SFGs can be used to describe systems without using equations.
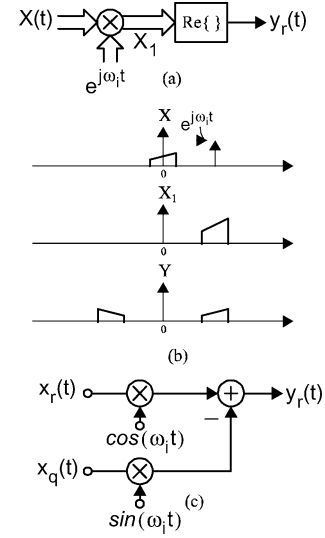

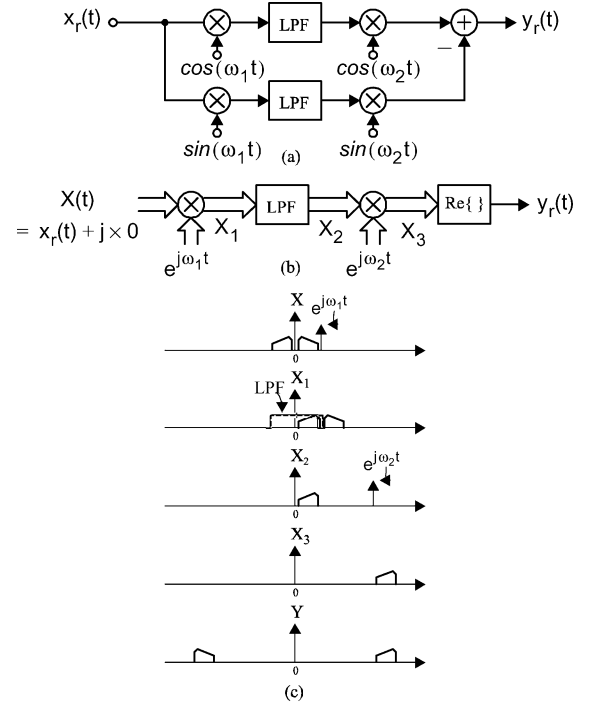Fig. 9. Image-reject up converter. (a) Complex SFG. (b) Example spectra. (c) Equivalent real SFG.

Fig. 10. Weaver method for SSB generation [15].

up so it is centered at ω_1. The lower sideband is then extracted using two real low-pass filters. The complex signal is then further frequency shifted to the desired RF frequency, in this case ω_2, and the imaginary part is discarded; the result is the final SSB signal at RF. The spectra of various locations of the complex SFG of Fig. 10(b) are shown in Fig. 10(c).

An alternative architecture for SSB generation, called Weaver's second method, replaces the first complex mixer and the low-pass filters with a complex PPF (or NPF), in order to extract the desired sideband directly before frequency shifting to the desired RF frequency.
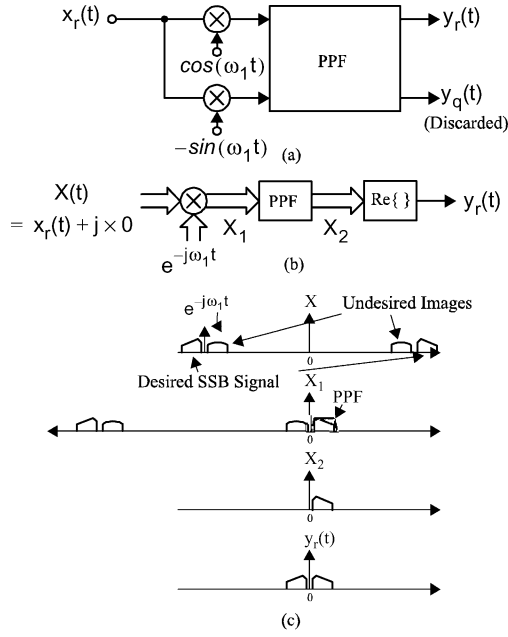
Fig. 11. Demodulating a SSB signal using the Hartley architecture [16].

D. SSB Receivers

An architecture closely related to SSB transmitters is an alternative for an SSB receiver based on using a PPF after a complex demodulation from RF. The PPF is used to attenuate the undesired sideband, as is shown in the real SFG of Fig. 11(a) and the equivalent complex SFG of Fig. 11(b).[5] From the plots of the spectra at different locations of the complex SFG, it is seen that the first complex mix frequency shifts the spectra so that the only significant components at positive frequencies are in the desired sideband. The sideband is extracted using a PPF. The final real demodulated output signal is obtained by simply taking the real output of the PPF and discarding its imaginary output. This approach was originally proposed by Hartley [16], where the PPF was implemented as two low-pass filters cascaded with simple RC phase-shift networks, as is shown in Fig. 12(a). An alternative means of realizing a wide-band passive PPF, that is less sensitive to component tolerances and is currently popular, uses the polyphase network shown in Fig. 12(b) [17]–[19]. The polyphase network is well analyzed in [19], where it is shown that it is an example of a complex filter obtained from frequency shifting a high-pass filter, as is discussed in Section IV.

E. Imaging Errors in Complex Mixers

Perhaps the major motivation for using image-reject or quadrature mixers is that they allow for frequency translation while minimizing the necessity for highly selective and sensitive image-reject filters at RF and IF frequencies. This is only true to the extent that quadrature mixers operate ideally. For example, if the complexoid that is modulating the input signal is quadrature imbalanced and has negative frequency components, then interferers can be imaged to fall in-band. The case of imaging errors due to quadrature imbalance in the channel is equivalent to a complex gain constant having

---

[5]This is a good example of using complex filtering to eliminate interfering images.
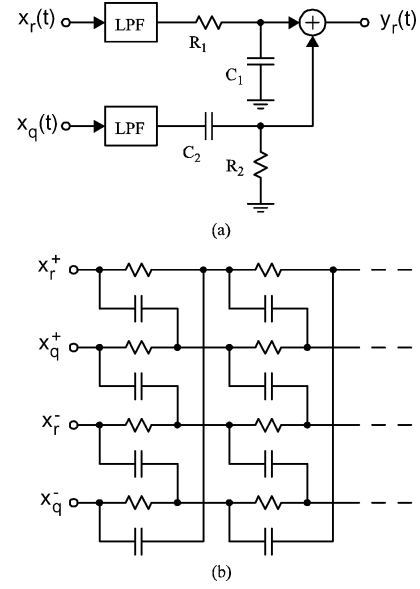

Fig. 12. (a) PPF used in the Hartley SSB receiver. (b) Polyphase approach for realizing a PPF [17].
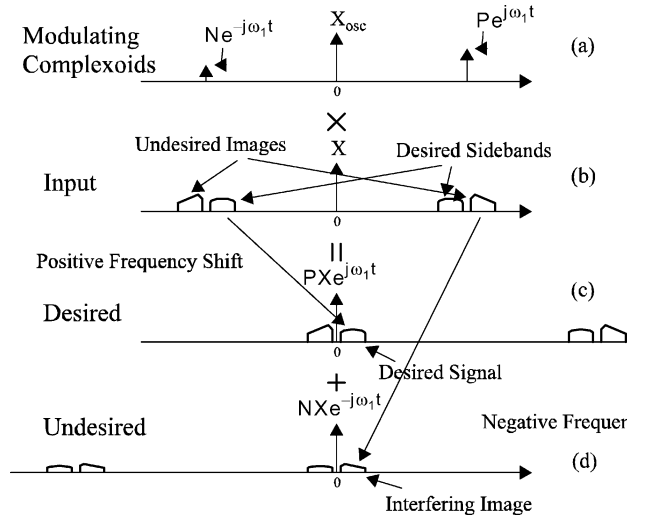

Fig. 13. Imaging due to a nonideal complexoid.

quadrature imbalance, and is discussed in Section IV.C. An in-depth and relatively complete analysis of imaging errors in complex mixers and quadrature samplers can be found in [20], which deals primarily with demodulating analog signals from a low-IF frequency to baseband. In this section, we discuss an example of demodulating a real carrier-frequency signal (or RF signal) to a low-IF frequency.

Consider the case of demodulating an SSB input signal, where the lower sideband is desired, for example. This case is similar to that in Fig. 11, but now the ideal demodulating complexoid, X_{osc}, is at a positive frequency. Assume that it is not ideal; we will show that this case results in there being a small modulating complexoid at a negative frequency as well, as shown in Fig. 13(a). The assumed input signal X is shown in Fig. 13(b). The desired frequency shift takes the the input signal and modulates it to more positive frequencies so that the lower sideband is just above dc, as is shown in Fig. 13(c). However, the smaller negative-frequency modulating complexoid in

addition, shifts the input signal to more negative frequencies so that the upper sideband, although attenuated, is sitting directly at the same frequency band as the desired lower sideband, as is shown in Fig. 13(d). The subsequent filtering by the PPF will output both the desired lower sideband and the interfering upper sideband image. For this reason, it is important to quantify the magnitude of the imaging complexoid (in this case at a negative frequency) as a function of the magnitude and phase errors of the modulating waveform.

Consider an ideal quadrature mixer having a multiplying complexoid given (using rectangular coordinates) as

$$x_{\mathrm{osc}}(t) = \cos(\omega_1 t) + j\sin(\omega_1 t). \qquad (16)$$

If we assume there are phase and magnitude errors, we can express the modulating waveform in a simplified form of (8) as

$$x_{\mathrm{osc}}(t) = \cos(\omega_1 t) + j(1+\varepsilon)\sin(\omega_1 t + \phi) \qquad (17)$$

where ε is the magnitude error and ϕ is the phase error. This assumes that we have normalized the complexoid so that the magnitude of the $\cos(\ )$ term is unity. We can now directly apply (10) and (11) to give

$$x_{\mathrm{osc}}(t) = Pe^{j\omega_1 t} + Ne^{-j\omega_1 t} \qquad (18)$$

where

$$P = \frac{A+B}{2} = \frac{1+(1+\varepsilon)e^{j\phi}}{2} \qquad (19)$$

and

$$N = \frac{A-B}{2} = \frac{1-(1+\varepsilon)e^{-j\phi}}{2}. \qquad (20)$$

For $\varepsilon, \phi \ll 1$, we see that the positive frequency term is slightly changed in magnitude and phase. These errors are normally small and easy to compensate; however, the negative frequency complexoid, ideally zero, now has a multiplier given by

$$N \cong \frac{1-(1+\varepsilon)(1-j\phi)}{2}$$
$$\cong -\frac{\varepsilon}{2} + j\frac{\phi}{2} \qquad (21)$$

which is also the multiplier for the final resulting images. It might be mentioned that (21) is the basis for a proposed adaptive quadrature mixer to be described later.

IV. COMPLEX FILTERS

In addition to image-reject mixers, complex filters are important and widely used signal processing blocks in modern wireless transceivers [47]. Complex filters use cross coupling between the real and imaginary signal paths in order to realize asymmetrical (in the frequency domain) filters having transfer functions that do not have the conjugate symmetry of real filters. This implies that their transfer functions have complex coefficients. The PPFs described previously can be considered a special case of complex filters. Complex filters can be realized using the basic operations of addition and multiplication, and the delay operator for discrete-time digital filters or the integrator operator for continuous-time analog filters.
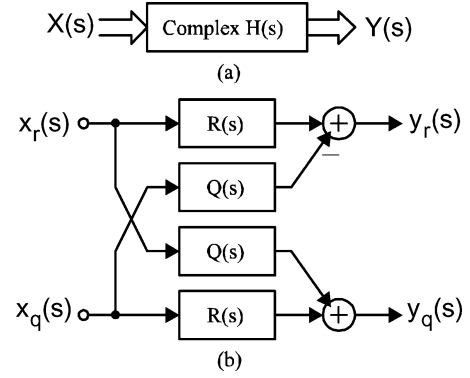

Fig. 14. Realizing a complex filter $H(s) = R(s) + jQ(s)$ by real SFG transfer filters $R(s)$ and $Q(s)$.

Complex analog transfer functions can be realized by either frequency-translating real filters [1], [2], [10], or by employing a direct method for deriving transfer complex functions to match asymmetrical specifications using procedures similar to those used for real filters [1], [8], [21]. Similar choices exist for obtaining suitable transfer functions for digital filters [2]–[4], [22]–[26]. In this tutorial introduction, complex filters derived using real-to-complex transformations are emphasized[6], for reasons of brevity. For the same reason, we limit our discussions to polyphase filters, active-RC filters, integrator-based filters, and delay-based digital filters.

A complex transfer function can be realized by using four real SFG filters [1], [12], as is shown in Fig. 14 for analog filters. An identical realization is possible for digital filters where the transfer functions are functions of z. For Fig. 14, we have

$$R(s) = \frac{H(s) + H^*(s)}{2} \qquad (22)$$

and

$$jQ(s) = \frac{H(s) - H^*(s)}{2}. \qquad (23)$$

When the filters leading from the real and imaginary branches of Fig. 14 do not exactly match, imaging errors (plus less harmful magnitude response errors) occur as we shall see

A. Frequency-Translated Analog Filters

One method for deriving complex transfer functions is to employ a complex substitution for the Laplace variable s. For example, to effect a positive frequency shift, one uses the substitution

$$s \rightarrow s - j\omega_0. \qquad (24)$$

The effect of this substitution on a low-pass filter is shown in Fig. 15. Thus, one can replace the procedure for realizing a PPF filter via a Hilbert transform, as is shown in Fig. 7, with the more general procedure for designing a complex filter that has a passband restricted to the desired (possibly positive) frequencies.
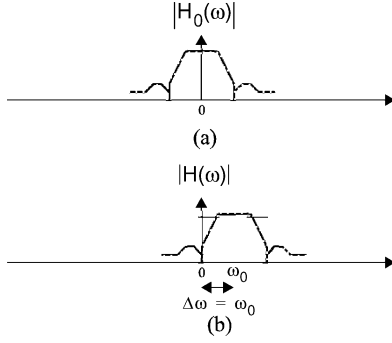
Fig. 15. (a) Baseband prototype magnitude filter response. (b) Magnitude response of a complex filter obtained by the substitution $s \rightarrow s - j\omega_0$.
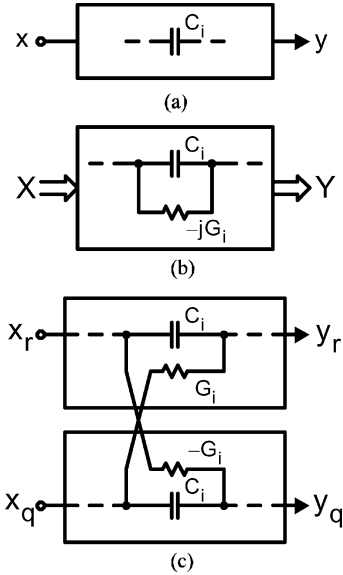

Fig. 16. (a) Capacitor in the real prototype filter. (b) Transformed capacitor in the complex filter. (c) Real-component realization of the complex capacitor.

A method for realizing complex analog filters is to start with an active *RC* prototype filter and then transform it to a complex frequency-translated filter; the procedure to do this is simple.

1) First, use an active *RC* prototype filter that is fully-differential. This is used to make the realization of negative components trivial.
2) Secondly, replicate exactly the prototype filter in order to realize the signal path for the imaginary signal components.
3) Finally, add cross-coupled resistors for each capacitor. The size and signs of these resistors determine the frequency translation.

To understand why this procedure works, consider first that 2) transforms the real prototype filter to a complex conjugate symmetric filter at the same frequencies as the prototype filter. To understand how the cross-coupling resistors result in the frequency translation, consider Fig. 16. Fig. 16(a) shows one of the capacitors in a complex filter at the same frequencies as the real prototype filter. Applying the frequency translation

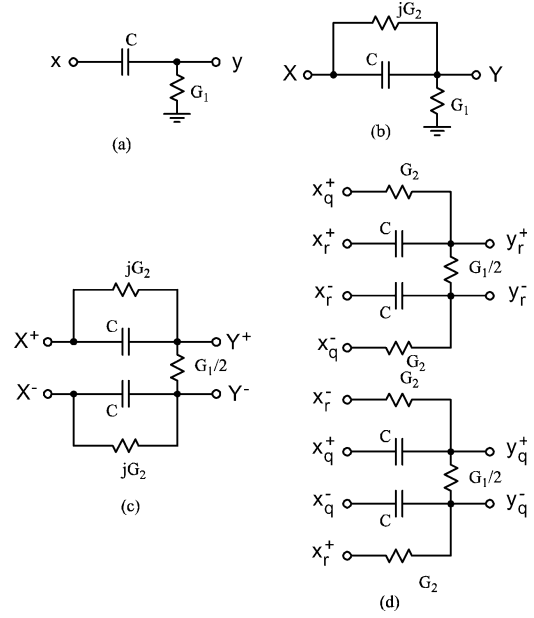$$s \rightarrow s - j\omega_0 \qquad (25)$$

Fig. 17. Using a complex frequency translation to realize a PPF. (a) High-pass prototype. (b) Complex band-stop having a complex admittance. (c) Fully-differential version of (b). (d) Replacing the complex admittances with cross-coupled real admittances between the real and imaginary paths.

results in transforming the capacitor to an admittance of a capacitor (of the same size) in parallel with an imaginary resistor of size $-j\omega_0 C$ according to the substitution

$$sC \rightarrow sC - j\omega_0 C. \qquad (26)$$

This is shown in Fig. 16(b) where

$$G_i = \omega_0 C_i. \qquad (27)$$

In order to realize the complex filter using real components, two identical real filters are used with cross-coupling, as is shown in Fig. 16(c). The negative cross-coupled resistor can be realized using fully differential circuits.

An example of the use of this complex frequency translation is a derivation of a polyphase network.[7] Consider the passive *RC* high-pass filter shown in Fig. 17(a). In this example, the transmission zero at dc will be frequency shifted to negative frequencies, so we use the substitution $s \rightarrow s + j\omega_0$. Letting

$$\omega_0 = \frac{G_2}{C} \qquad (28)$$

gives the required substitution as

$$sC \rightarrow sC + jG_2. \qquad (29)$$

Thus, the complex frequency-shifted high-pass is now as shown in Fig. 17(b). A fully-differential version of the circuit of Fig. 17(b) is shown in Fig. 17(c). This complex filter can be realized by two parallel real filters with cross-coupled resistors, as is shown in Fig. 17(d). Upon examination, this circuit is seen to be same as the polyphase network of Fig. 12(b) except for the inclusion of load resistors $G_1/2$ in Fig. 17(d). Taking $G_1 = 0$ would result in very narrow notches. Normally, polyphase networks are intended to be cascaded [17], [19], and the load

[7]The derivation presented here is an alternative to that presented in [19].
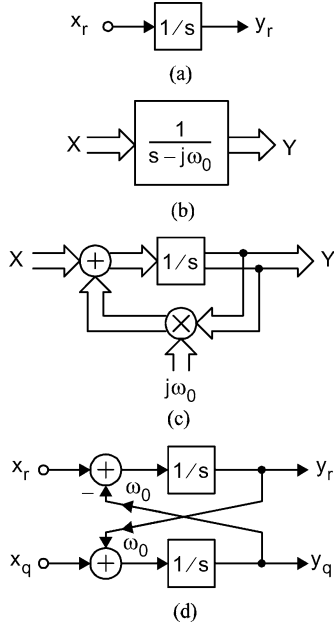
Fig. 18. Frequency shifting a real integrator to a complex positive-frequency integrator.

Fig. 19. Frequency shifting a real delay operator to a complex positive frequency.

on each section is the succeeding section, as is discussed in depth in [19].

An alternative procedure for realizing continuous-time complex filters is based on frequency-translating SFG prototype filters which are based on integrators [1]. This procedure is illustrated by applying it to the single integrator shown in Fig. 18(a). In Fig. 18(b) and (c) are shown complex SFGs that realize the frequency-shifted integrator. The complex SFG of Fig. 18(c) is converted to the equivalent real SFG of Fig. 18(d), where the necessary cross-coupling is explicit. The procedure for frequency shifting any real SFG integrator-based filter is simply: 1) replicate the real SFG filter for the imaginary path; and 2) cross couple at each integrator, as is shown in Fig. 18(d). The strength of the cross-couplings determine the frequency of the shift. As always, this cross coupling is simplified by using fully-differential circuits.

B. Frequency-Translated Digital Filters

Complex discrete-time and digital filters are as essential to modern wireless systems as the complex analog blocks already described. For example, digital complex filters are used as decimation filters for complex A/Ds, and also as band-limiting filters at baseband for spectral shaping (i.e., Nyquist filters, such as root raised-cosine filters, designed to minimize inter-symbol interference). An approach can be used for frequency shifting real discrete-time delay-based digital filters to complex asymmetrical filters [2] that is similar to the one that was used for analog filters. Consider the real delay operator

$$z^{-1} = e^{-j\omega T} \tag{30}$$

undergoing a frequency shift by applying the variable substitution
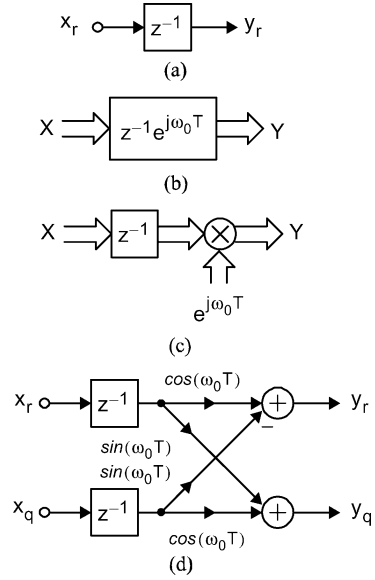
$$\omega \rightarrow \omega - \omega_0. \tag{31}$$

We have

$$e^{-j\omega T} \rightarrow e^{-j(\omega-\omega_0)T} = z^{-1}e^{j\omega_0 T}. \tag{32}$$

Thus, discrete-time filters can be transformed by once again replicating the filter for the imaginary path and then placing a complex-coefficient multiplier directly after every delay operator, as is shown in Fig. 19. It is obvious that this approach can be used to realize complex filters that have their frequency-shifts programmable. As an additional note, the complex rotation implied by the multiplication by $e^{j\omega_0 T}$ is called a *Cordic* operation, and its realization has been well studied [27], [28].

Some special cases of frequency-shifted discrete-time filters are worth mentioning. For example, some discrete-time filters are based on using as fundamental building blocks *Euler forward* and *backward-difference integrators* [29], which are often called *lossless digital integrators* [30]; these are bases for many switched-capacitor (SC) filter realizations. The filters before frequency translation have unity-gain feedback around the delay operators. After translation, it is desirable to preserve this unity-gain feedback in order to facilitate their realization using SC integrators as the fundamental building blocks. This is possible as shown in the original and transformed discrete-time integrators in Fig. 20. The Realization of the complex SFGs in Fig. 20(b) and (d) using real SFGs is straightforward.

Another interesting special case is when the frequency shift is by $e^{j\omega_0 T}$, where $f_0 = k\omega_0/2\pi$ is equal to some multiple $k/4$ times the sampling frequency. For this case, we have

$$e^{jk\omega_0 T} = e^{jk(\pi/2)} = j^k. \tag{33}$$

Using Fig. 4. with (33), we see that frequency shifting by $k/4$ times the sampling frequency can be realized without multipliers, just by using a path interchange and a signal inversion; this is a considerable simplification. As an example of using this transform, consider using as a prototype filter a first-order digital differentiator that has a notch or transmission zero at dc. This prototype filter has a real transfer function given by
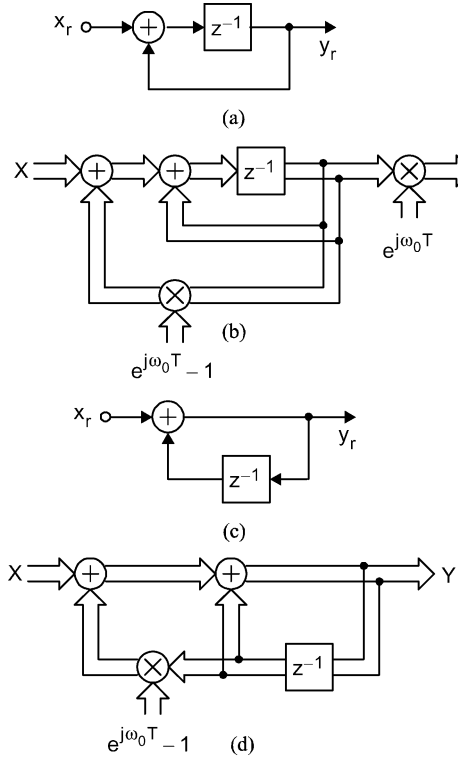
$$H_0(z) = 1 - z^{-1}. \tag{34}$$

Fig. 20. Frequency translating (a) Forward-difference integrator. (c) Backward- difference integrators to complex discrete-time integrators.
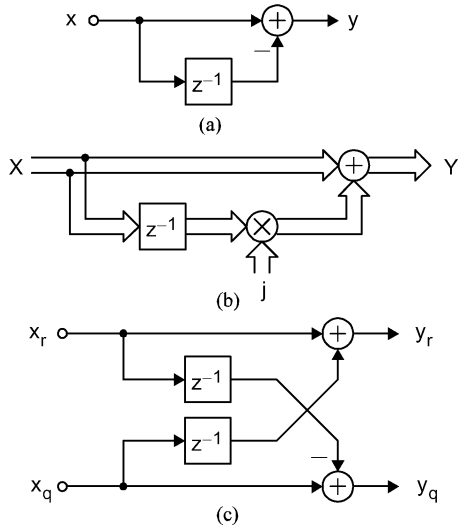

Fig. 21. (a) Prototype filter with a notch at dc. (b) Complex frequency-shifted filter with a notch at $f_s/4$. (c) Its realization using real SFGs.

Its SFG is shown in Fig. 21. If this prototype filter, with a notch at dc is frequency shifted to a complex filter with a notch at $f_s/4$, then, its new transfer function is given by

$$H(z) = 1 - jz^{-1}. \tag{35}$$

The complex SFG of this transfer function is shown in Fig. 21(b), and its realization using real SFGs is shown in Fig. 21(c). For practical purposes, this filter is the same as that proposed in [31], where a number of these filters were cascaded in order to give wider notch bandwidths. Another
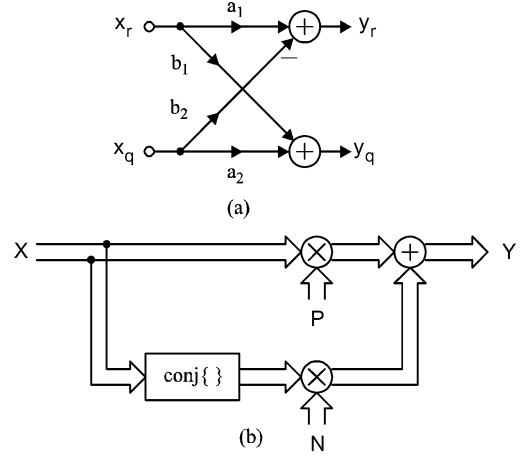

Fig. 22. (a) Generalized multiplication where a_1, b_1 are not necessarily equal to a_2, b_2. (b) Equivalent complex SFG.

example of realizing a simplified complex notch filter at 1/4 the sampling frequency, with a transfer function given by (35), is described in [20]. In this case, a discrete-time complex analog filter/mixer combination was realized at the input of a pair of baseband oversampling A/D converters by time multiplexing some switched capacitors using a modified switch arrangement, a simple yet effective architecture. Other examples of frequency translated complex filters are filter banks. This area has been extensively researched and described in the literature and is outside the scope of this publication. However, one possible approach developed by the author that has good step-band offered performance is described in [32] and mentioned as an example.

C. Imaging Errors in Complex Multipliers and Transfer Functions

The analysis of imaging errors due to real coefficient errors in complex multipliers and transfer functions is similar to that presented in Section III.E for complex mixers. Consider a generalized multiplication function as shown in Fig. 22(a) where, ideally for a complex multiplication $a_1 = a_2$ and $b_1 = b_2$, but, in the case of mismatch and quadrature imbalance, this is not true. Assuming

$$P = \frac{a_1 + a_2}{2} + j\frac{b_1 + b_2}{2} \tag{36}$$

and

$$N = \frac{a_1 - a_2}{2} + j\frac{b_1 - b_2}{2} \tag{37}$$

then it is straightforward to show that Fig. 22(b) is equivalent to Fig. 22(a). Using (6) and (7), we see that real coefficient errors result in the additional complexoids in the signal path at the opposite frequencies of the multiplier input complexoids; positive frequency signal components are both transmitted and also shifted to negative frequencies, and vice versa, with the magnitude of these imaging components being proportional to the *differences* of the real coefficients. For example, in-band signal components can result in additional complexoids in the stopband. Also, out-of-band interferers can result in additional components in the passband. If these coefficient errors occur

at multipliers inside digital filters, then these imaging components are generated at the output of each nonideal multiplier. The imaging components are then filtered by the transfer functions from the multiplier outputs to the filter outputs and subsequently appear as imaging errors at the filter output. To minimize signal-to-stopband errors, one should design in order to have out-of-band notches in the transfer functions from the multiplier outputs to the filter output [33]. In addition, to minimize interferer-to-signal errors, one should design to have out-of-band notches in the transfer function from the filter input to the inputs of the multipliers. These situations can be quantified using the intermediate-function analysis approach described in [1], this is a good area for future research. An example of the application of these considerations is in the filter design described in [52].

A similar situation occurs when realizing complex filters using the approach in Fig. 14(b), where we now have nonmatched filters $R_1(s)$, $R_2(s)$, $Q_1(s)$, and $Q_2(s)$. The nontranslated frequency components are filtered by the *average* transfer functions

$$H_{\text{avg}}(s) = \frac{R_1(s) + R_2(s)}{2} + j\frac{Q_1(s) + Q_2(s)}{2} \qquad (38)$$

whereas imaging components are produced (both in-band and out-of-band) by first *conjugating* the input signals, which changes the signs of the frequencies of the spectral components, and then filtering these images by the difference transfer functions [1].

$$H_{\text{diff}}(s) = \frac{R_1(s) - R_2(s)}{2} + j\frac{Q_1(s) - Q_2(s)}{2}. \qquad (39)$$

In this case, the images occur directly at the filter outputs, and there is less freedom to minimize images by careful choice of the intermediate transfer functions, as compared to the situation where filters are cross coupled internally.

V. RECENT APPLICATIONS OF COMPLEX SIGNAL PROCESSING

A. Adaptive Quadrature Mixers

Many recent wireless receivers tune or adapt the systems to eliminate image errors due to nonideal quadrature mixers. This tuning can be done in either the analog or the digital domain.

As a preliminary to discussing adaptive algorithms, note that most complex adaptive systems require the output of a sensitivity filter, $s(t)$, which is correlated with an error $e(t)$, in order to drive the error to zero. A possible update algorithm is given by

$$\Delta k_i = -\mu \langle e, s \rangle \qquad (40)$$

where μ is a small constant controlling the update rate. Often, this update is approximated using the stochastic instantaneous update to give

$$k_i(n) = k_i(n-1) - \mu e(n)s^*(n). \qquad (41)$$

Note that $s^*(n)$ is conjugated for complex signals. Alternatively, $e(n)$ could have been conjugated. The required sensitivity filter, $s(n)$, is often trivial for FIR systems, and often not very complicated even for IIR systems [34], [35] (and can be found using Tellegen's Theorem [51]).
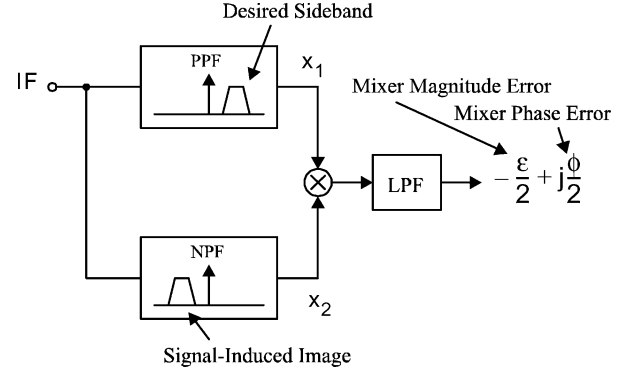

Fig. 23.   On-line system for obtaining the magnitude and phase mismatch errors of a quadrature mixer in a low-IF receiver.
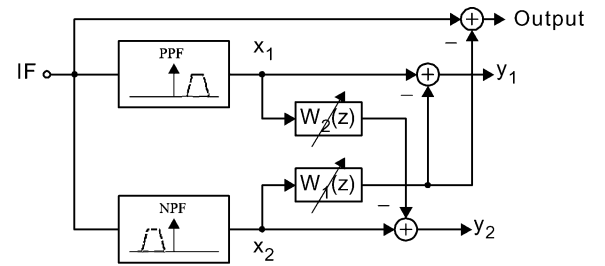

Fig. 24.   Digital adaptive filter approach for adapting a quadrature mixer [38].

A possible approach for adapting a quadrature mixer is based on (21). A block diagram showing how estimates for the magnitude and phase errors are found is shown in Fig. 23. In this approach, assume a quadrature-imbalanced mixer is used to demodulate an RF signal to a low IF. A complex PPF can be used to extract the desired signal. In addition, assume a NPF is used to extract the undesired signal-induced image at negative frequencies, which is caused by the magnitude and phase mis-match errors in the RF mixer. If the PPF and NPF complex outputs are correlated, that is, multiplied together and averaged (or low-pass filtered), then the approximate result is a complex dc signal given by (21). Thus, the real output of the multiplication can be used to drive the gain error to zero, and the imaginary part can be used to drive the phase errors to zero. This assumes the errors are wide band and frequency independent. In normal practice, the signal processing for the filtering and correlation would be done in the digital domain, but the tuning would be done in the analog domain at the mixers. Interferers would thus be eliminated before the A/D conversion, and this would help prevent overloading the A/D and preceding preamplifiers. The approach just proposed is similar to that described in [36], except that in [36], the adaptation was done with an interferer only used as a reference input, the error functions minimized were different, and the adaptation update was performed in the analog domain.

Alternative approaches, where the signal processing and the tuning are both done in the digital domain, are described in [37], [38], with a realization based on [38] described in [39]. This approach is shown in Fig. 24. As in the previous approach, a complex PPF is used to extract the desired signal, and a second NPF is used to extract the images. The fundamental idea on which this approach is based is that a symmetric decorrelating filter is
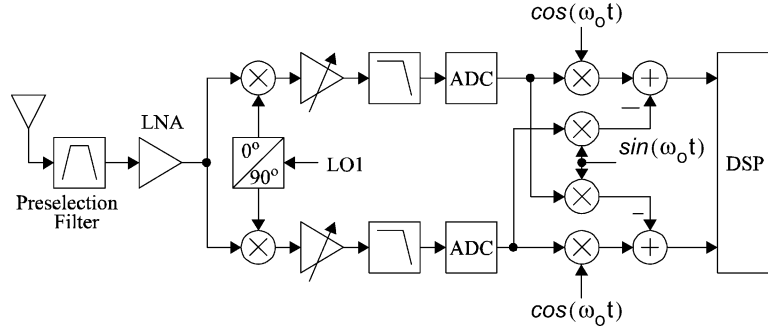
Fig. 25.   Low-IF architecture for a receiver.

used to minimize image components in y_1 and signal components in y_2 [40]. This helps to minimize biases. Another advantage of this approach is that *frequency-dependent* imaging errors are cancelled as well. A recently proposed algorithm [41], although completely implemented in the digital domain, does include some features of both of the above algorithms. Another interesting adaptive image-reject approach, that, again, is completely in the digital domain, is based on blind source separation compensation [42].

The alternatives described are just the beginning of what is expected to be a fruitful area of research. One future possibility is to use to image cancellers, one in the analog domain and a second canceller in the digital domain. Tuning the mixer inputs in the analog domain is useful in preventing overload in the IF stages and in helping to attain timing acquisition, but is useful only for correcting frequency-independent errors. A second adaptive fine tuning in the digital domain similar to [38] can be used to further eliminate frequency-dependent errors of, for example, complex oversampling A/Ds used at the IF.

B. Low-IF Receivers

A currently popular architecture for realizing highly integrated, moderately wide-band, wireless transceivers is the low-IF architecture [45]–[47]. An example of a low-IF receiver is shown in Fig. 25. In a low-IF receiver, the RF signal is demodulated to baseband in two stages; the first stage is a standard quadrature mixer with a real input signal that requires two real analog multipliers. This translates the RF input signal down to a low-IF frequency. The high-IF component after the first shift is eliminated by low-pass filters; at that point a second complex mixer is used to shift the low-IF signal to baseband. The second complex mixer requires four real multipliers. These can be realized using analog multipliers as in [46]. Alternatively, the A/D conversion can be done at the IF stage, as is shown in Fig. 25, and then the second complex frequency shift can be realized in the digital domain [47]. This allows the second complex modulation to be almost ideal. Also, if the A/D sampling frequency is chosen to be a small multiple of the IF frequency, then the second mix is significantly simplified. For example, if the sampling frequency is four times the IF frequency, then the oscillator inputs to the second complex digital mixer are simply ± 1 or 0. This digital modulation alternative is often preferable.

Low-IF architectures are especially suitable for multistandard receivers when the channel-selection filters are realized after the A/D converters, using digital circuits, and, thus, can
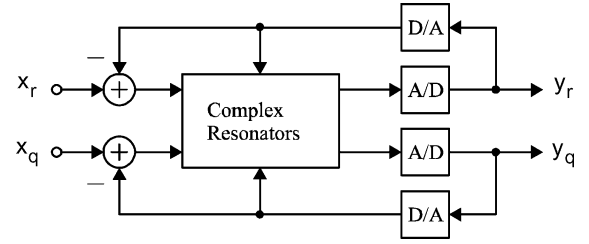
Fig. 26.   Complex $\Delta\Sigma$ oversampling A/D converter architecture.

be programmed to accommodate the requirements of the different standards. The low-IF architectures greatly minimize dc offset errors due to feedback of the local-oscillator (LO) and the large $1/f$ noise of MOS transistors. The low-IF architectures do suffer from images when the IF frequency is low, but these can be significantly minimized by using even relatively simple complex filters at the IF [47], [20].

In general, when the A/D conversion occurs before the channel-selection filters, then the A/D conversion must necessarily be high dynamic range, and *the A/D converter is almost always the limiting factor determining the maximum achievable data rate of the receiver*. Assuming the A/D converter is the limiting factor on the maximum achievable data rate, then it is possible to improve significantly the maximum-achievable data rate using the modulation approach proposed in [49]. A typical low-IF architecture has IF spectral components at positive or negative frequencies only; this wastes half the available bandwidth of the A/Ds.[8] It is possible to send additional data in the unused frequency band. In the simplest implementation, one channel is implemented at positive frequencies, and one channel is implemented at negative frequencies (as proposed in [49]); in more advanced realizations, multiple channels are implemented at both positive and negative frequencies using orthogonal-frequency-division-multiplexing (OFDM) techniques. In both cases, the physical hardware is the same as that used for typical low-IF receivers (as shown in Fig. 25); the increase in complexity is all in the digital domain and is quite feasible for current data rates.

For example, consider the approach for two channels only, one at positive and one at negative frequencies. At the transmitter, two simultaneous quadrature input channels are used; one is modulated to positive frequencies, and one is modulated

---

[8]This assumes that the A/D converters are not complex oversampling A/Ds; if they are, the bandwidth is not necessarily wasted. This is one of the motivations for using complex oversampling A/Ds.
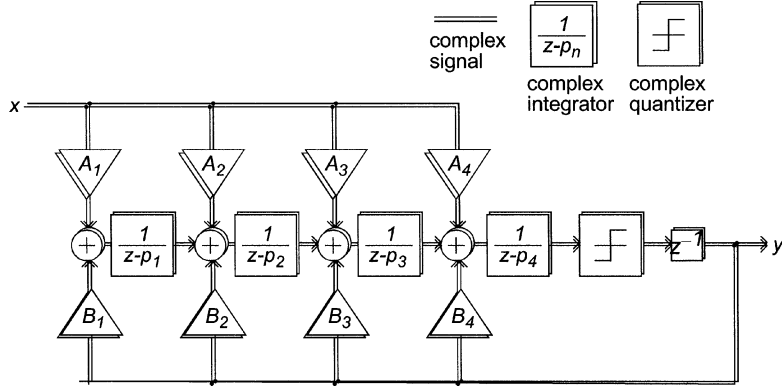
Fig. 27. Complex SFG of fourth-order quadrature $\Delta\Sigma$ modulator from [52].

to negative frequencies using quadrature mixers in the digital domain. A guardband is left at dc. The combined signal is then modulated up to the RF and transmitted. The conversion to the analog domain can occur just before or after the last modulation. This approach is much like a double SSB system where both an upper and a lower sideband are transmitted together (sometimes called a suppressed-carrier modulation system). At the receiver, the RF signal is demodulated so that one channel is again at a low positive IF, and the second channel is at a low negative IF. The IF signal is then digitized using two A/D converters in a manner similar to that used in a typical low-IF receiver. After the A/D conversion, the individual channels can be independently demodulated using complex signal processing in the digital domain. This architecture results in a guardband at dc which allows the IF signal to be ac coupled, and this minimizes errors due to the local feedback of the RF oscillator (LO feedback) and $1/f$ noise, similar to the traditional low-IF architecture, *yet it supports almost twice the data rate for a given sampling frequency at the A/D converter with no increase in hardware complexity.*

C. Complex and Quadrature Oversampling A/D Converters

All signal processing blocks preceding the channel-selection filters in a receiver must be high dynamic range. Typical specifications are linearities equivalent to 14-bit ideal A/D converters or more, that is, in excess of 86-dB SNDR. Typical specifications for the analog bandwidths are now in excess of 2 MHz and as high as 5 MHz. Realizing A/D converters that can meet these demanding specifications is a challenging task. A possible architecture that is gaining in popularity for this application is the complex oversampling A/D converter [8]. Complex oversampling $\Delta\Sigma$ A/D converters combine the complex filtering ideas of [1] and the real bandpass oversampling $\Delta\Sigma$ A/D converters of [50]. By using a complex filter in the $\Delta\Sigma$ loop, the effective signal bandwidth is cut in half, and this doubles the oversampling ratio (OSR). The result, ideally, is a much-improved signal-to-noise distortion ratio (SNDR) [51], [52], depending on the order of the oversampling loop and the resolution of the D/As embedded in the A/D. Also, it is possible to choose the locations of the zeros in the noise-transfer function (NTF) in order to minimize errors due to quantization effects [33]. Another result is that the zeros of the signal-transfer function (STF) can be independently chosen to filter out images from an imperfect preceding quadrature mixer. Thus, complex image-reject filtering
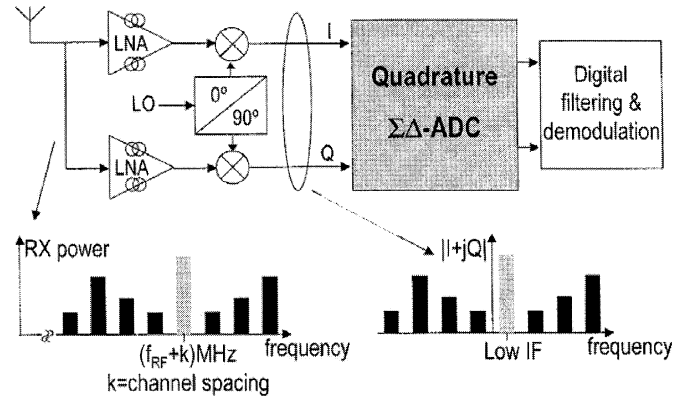

Fig. 28. Using a quadrature $\Delta\Sigma$ modulator to digitize an IF signal [52], [54].

and the A/D conversion are effectively combined in a single unit. The basic architecture of the complex oversampling $\Delta\Sigma$ A/D converter is shown in Fig. 26.

In [52], a fourth-order complex, that is eighth-order real, oversampling A/D, that used 1-bit internal converters, was reported. A complex SFG of the architecture showing the complex resonators is shown in Fig. 27. It should be noted that each of the p_i coefficients is complex, thus each block having a transfer function

$$H_i = \frac{1}{z - p_i} \tag{42}$$

realizes a complex resonator close to the desired IF frequency. The design of the internal complex resonator-based filter was done to maximize SNDR by careful choice of the NTF and STF transmission zeros [33]. The converter was implemented using SC circuits. This first-integrated quadrature $\Delta\Sigma$ converter had a measured SNDR of 65 dB for a 100-kHz signal bandwidth. The converter was also verified to have better stability properties than real oversampling converters.

Recently, examples of continuous-time complex $\Delta\Sigma$ A/D converters have also been reported [53], [54]. For example, a converter intended to be used to digitize an IF signal of a wireless receiver, similar to [52] is reported in [54]. This application is shown in Fig. 28. A functional block diagram of the converter of [54] is shown in Fig. 29. The A/D converter exhibited an SNDR of 76 dB for a 1-MHz signal bandwidth,
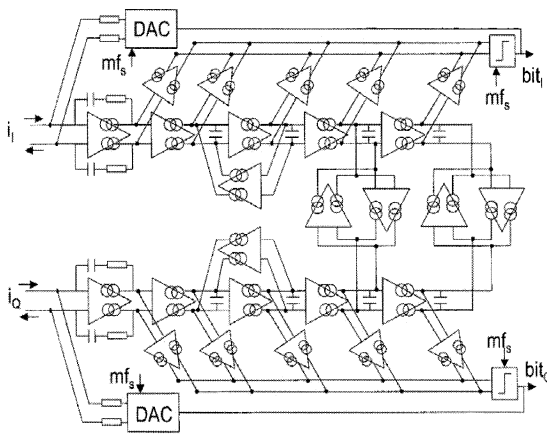
Fig. 29. Block diagram of complex $\Delta\Sigma$ modulator of [54].

yet dissipated only 4.4 mW. These results are excellent at the time of publication.

Currently, there has been little published on how best to implement the complex digital filters required that must be included following the analog modulators in order to attenuate quantization noise and allow the signals to be decimated. These can be realized directly at the IF frequencies, or the IF signals can first be demodulated to baseband using a complex mixer, and then the decimation filters can be realized at baseband. This is expected to be an active area for future research.

VI. CONCLUSION

A tutorial description of the use of complex signal processing in wireless systems has been presented. First, the fundamentals have been explained and then their use in a number of applications has been described. A highly graphical SFG approach has been used throughout. Example applications of complex mixers, filters, low-IF receivers, and complex oversampling A/D converters have been described.

REFERENCES

[1] W. M. Snelgrove, "Intermediate function synthesis," Ph.D. dissertation, Univ. Toronto, Toronto, ON, Canada, 1982.

[2] T. H. Crystal and L. Ehrman, "The design and applications of digital filters with complex coefficients," *IEEE Trans. Audio Electroacoust.*, vol. AU-16, no. 3, pp. 315–320, Sept. 1968.

[3] R. Boite and H. Leich, "On digital filters with complex coefficients," in *Network and Signal Theory*, J. K. Skwirzynski and J. O. Scanlan, Eds. London, U.K.: Peter Peregrinus, 1973, pp. 344–351.

[4] M. T. McCallig, "Design of digital FIR filters with complex conjugate pulse responses," *IEEE Trans. Circuits Syst.*, vol. CAS-25, pp. 1103–1105, Dec. 1978.

[5] A. V. Oppenheim and R. W. Schafer, *Digital Signal Processing*. Englewood Cliffs, NJ: Prentice-Hall, 1975.

[6] W. M. Snelgrove and A. S. Sedra, "State-space synthesis of complex analog filters," in *Proc. Eur Conf. Circuit Theory and Design*, 1981, pp. 420–424.

[7] G. R. Lang and P. O. Brackett, "Complex analogue filters," in *Proc. Eur Conf. Circuit Theory and Design*, 1981, pp. 412–419.

[8] W. M. Snelgrove, A. S. Sedra, G. R. Lang, and P. O. Brackett. (1981) Complex analog filters. Univ. Toronto, Toronto, ON, Canada. [Online]. Available: ftp://ftp.eecg.toronto.edu/pub/software/martin/snelgrove_cmplx.pdf

[9] R. Allen, "Complex analog filters obtained from shifted lowpass prototypes," M.A.Sc. thesis, Univ. Toronto, Toronto, ON, Canada, 1985.

[10] A. Sedra, W. Snelgrove, and R. Allen, "Complex analog bandpass filters designed by linearly shifting real low-pass prototypes," in *Proc. Int. Symp. Circuits and Systems*, vol. 3, 1985, pp. 1223–1226.

[11] Q. Liu, "Switched-capacitor complex filters," M.A.Sc. thesis, Univ. Toronto, Toronto, ON, Canada, 1985.

[12] E. A. Lee and D. G. Messerschmitt, *Digital Communication*. Boston, MA: Kluwer Academic, 1988.

[13] J. Crols and M. Steyaert, *CMOS Wireless Transceiver Design*. Boston, MA: Kluwer Academic, 1997.

[14] B. Razavi, *RF Microelectronics*. Englewood Cliffs, NJ: Prentice-Hall, 1998.

[15] D. K. Weaver, Jr., "A third method of generation and detection of single-sideband signals," *Proc. IRE*, pp. 1703–1705, June 1956.

[16] R. Hartley, "Modulation System," U.S. Patent 1 666 206, Apr. 1928.

[17] M. J. Gingell, "Single-Sideband modulation using sequence asymmetric polyphase networks," *Elect. Commun.*, vol. 48, no. 1-2, pp. 21–25, 1973.

[18] J. Crols and M. Steyaert, "An analog integrated polyphase filter for a high-performance low-IF receiver," in *Proc. VLSI Circuits Symp.*, Kyoto, Japan, June 1995, pp. 87–88.

[19] F. Behbahani, Y. Kishigami, J. Leete, and A. Abidi, "CMOS mixers and polyphase filters for large image rejection," *IEEE J. Solid-State Circuits*, vol. 36, pp. 873–887, June 2001.

[20] K.-P. Pun, J. E. Franca, C. Azeredo-Leme, and R. Reis, "Quadrature sampling schemes with improved image rejection," *IEEE Trans. Circuits Syst. II*, vol. 50, pp. 641–648, Sept. 2003.

[21] C. Cuypers, N. Voo, M. Teplechuk, and J. Sewell, "The general synthesis of complex analogue filters," in *Proc. Int. Conf. Electricity, Circuits, Systems*, vol. 1, 2002, pp. 153–156.

[22] A. Fettweis, "Principles of complex wave digital filters," *Int. J. Circuit Theory Applicat.*, vol. 9, pp. 119–134, 1981.

[23] X. Chen and T. W. Parks, "Design of FIR filters in the complex domain," *IEEE Trans. Acoust., Speech, Signal Processing*, vol. 35, pp. 144–153, Feb. 1987.

[24] P. Regalia, S. Mitra, and J. Fadavi-Ardekani, "Implementation of real coefficient digital filters using complex arithmetic," *IEEE Trans. Circuits Syst.*, vol. CAS-34, pp. 345–353, Apr. 1987.

[25] X. Chen and T. Parks, "Design of IIR filters in the complex domain," *IEEE Trans. Acoust., Speech, Signal Processing*, vol. 38, pp. 910–920, June 1990.

[26] M. Komodromos, S. Russell, and P. T. P. Tang, "Design of FIR filters with complex desired frequency response using a generalized remez algorithm," *IEEE Trans. Circuits Syst. II*, vol. 42, pp. 428–435, Apr. 1995.

[27] J. Volder, "The CORDIC trigometric computing technique," *IEEE Trans. Comput.*, vol. EC-8, pp. 330–334, Sept. 1959.

[28] A. Madisetti, A. Kwentus, and A. N. Willson, Jr., "A 100-MHz 16-b direct digital frequency synthesizer with a 100-dBc spurious-free dynamic range," *IEEE J. Solid-State Circuits*, vol. 34, pp. 1399–1410, Aug. 1999.

[29] L. R. Rabiner and B. Gold, *Theory and Application of Digital Signal Processing*. Englewood Cliffs, NJ: Prentice-Hall, 1975.

[30] L. T. Bruton, "Low-sensitivity digital ladder filters," *IEEE Trans. Circuits Syst.*, vol. CAS-22, pp. 168–176, Mar. 1975.

[31] S. Levantino, C. Samori, M. Banu, J. Glas, and V. Boccuzzi, "A CMOS GSM IF-sampling circuit with reduced in-channel aliasing," *IEEE J. Solid-State Circuits*, vol. 38, pp. 895–904, June 2003.

[32] K. W. Martin, "Small side-lobe filter design for data communication applications," *IEEE Trans. Circuits Syst. II*, vol. 45, pp. 1155–1161, Aug. 1998.

[33] S. Jantzi, K. Martin, and A. S. Sedra, "The effects of mismatch in complex bandpass $\Sigma\Delta$ modulators," in *Proc. IEEE Int. Symp. Circuits and Systems (ISCAS'96)*, May 1996, pp. 227–230.

[34] K. Martin and M. T. Sun, "Adaptive filters suitable for real-time spectral analysis," *IEEE Trans. Circuits Syst.*, vol. CAS-33, pp. 218–229, Feb. 1986.

[35] T. Kwan and K. Martin, "Adaptive detection and enhancement of multiple sinusoids using a cascade IIR filter," *IEEE Trans. Circuits Syst.*, vol. 36, pp. 937–947, July 1989.

[36] L. Der and B. Razavi, "A 2-GHz CMOS image-reject receiver with LMS calibration," *IEEE J. Solid-State Circuits*, vol. 38, pp. 167–175, Feb. 2003.

[37] J. Paez-Borrallo and F. J. C. Quiros, "Self adjusting digital image rejection receiver for mobile communications," in *Proc. IEEE Vehicular Technology Conf.*, vol. 2, May 1997, pp. 686–690.

[38] L. Yu and W. M. Snelgrove, "A novel adaptive mismatch cancellation system for quadrature IF radio receivers," *IEEE Trans. Circuits Syst. II*, vol. 46, pp. 789–801, June 1999.

[39] K. P. Pun, J. Franca, and C. Azeredo-Leme, "The correction of frequency-dependent I/Q mismatches in quadrature receivers by adaptive signal separation," in *Proc. IEEE Int. Symp. Circuits and Systems (ISCAS'01)*, 2001, pp. 424–427.

[40] D. V. Compernolle and S. V. Gerven, "Signal separation in a symmetric adaptive noise canceler by output decorrelation," *IEEE Trans. Signal Processing*, vol. 43, pp. 1602–1612, July 1995.

[41] C. C. Chen and C. C. Huang, "On the architecture and performance of a hybrid image rejection receiver," *IEEE J. Select. Areas Commun.*, vol. 19, pp. 1029–1040, June 2001.

[42] M. Valkama and M. Renfors, "Advanced methods for I/Q imbalance compensation in communication receivers," *IEEE Trans. Signal Processing*, vol. 49, pp. 2335–2344, Oct. 2001.

[43] A. A. Abidi, "Direct-conversion radio transceivers for digital communications," *IEEE J. Solid-State Circuits*, vol. 30, pp. 1399–1410, Dec. 1995.

[44] B. Razavi, "Design considerations for direct-conversion receivers," *IEEE Trans. Circuits Syst. II*, vol. 44, pp. 428–435, June 1997.

[45] J. Crols and M. S. J. Steyaert, "A single-chip 900 MHz CMOS receiver front-end with a high performance low-IF topology," *IEEE J. Solid-State Circuits*, vol. 30, pp. 1483–1492, Dec. 1995.

[46] J. C. Rudell, J. Ou, T. B. Cho, G. Chien, F. Brianti, J. A. Weldon, and P. R. Gray, "A 1.9-GHz wide-band IF double conversion CMOS receiver for cordless telephone applications," *IEEE J. Solid-State Circuits*, vol. 32, pp. 2071–2088, Dec. 1997.

[47] J. Crols and M. Steyaert, "Low-IF topologies for high-performance analog front ends of fully integrated receivers," *IEEE Trans. Circuits Syst. II*, vol. 45, pp. 269–282, Mar. 1998.

[48] K. P. Pun, J. E. Franca, and C. Azeredo-Leme, "A quadrature sampling scheme with improved image rejection for complex-IF receivers," in *Proc. IEEE Int. Symp. Circuits Systems (ISCAS'01)*, May 2001, pp. 45–48.

[49] S. Mirbbasi and K. Martin, "Hierarchical QAM: A spectrally efficient DC-free modulation scheme," *IEEE Commun. Mag.*, vol. 38, pp. 140–146, Nov. 2000.

[50] S. A. Jantzi, W. M. Snelgrove, and P. F. Ferguson, Jr., "A fourth-order bandpass sigma-delta modulator," *IEEE J. Solid-State Circuits*, vol. 28, pp. 282–291, Mar. 1993.

[51] S. Jantzi, "Quadrature bandpass delta-sigma modulation for digital radio," Ph.D. dissertation, Univ. Toronto, Toronto, ON, Canada, 1997.

[52] S. A. Jantzi, K. Martin, and A. S. Sedra, "Quadrature bandpass $\Delta\Sigma$ modulation for digital radio," *IEEE J. Solid-State Circuits*, vol. 32, pp. 1935–1949, Dec. 1997.

[53] F. Henkel *et al.*, "A 1 MHz-bandwidth second-order continuous-time quadrature bandpass sigma-delta modulator for low-IF receivers," in *Proc. IEEE Int. Solid-State Circuits Conf.*, Feb. 2002, pp. 214–215.

[54] K. Philips, "A 4.4 mW 76 dB complex $\Sigma\Delta$ ADC for bluetooth receivers," in *Proc. IEEE Int. Solid-State Circuits Conf.*, Feb. 2003, pp. 64–65.

Kenneth W. Martin (S'75–M'80–SM'89–F'91) received the B.A.Sc., M.A.Sc., and Ph.D. degrees from the University of Toronto, Toronto, ON, Canada, in 1975, 1977, and 1980, respectively.

From 1977 to 1978, he was a member of the Scientific Research Staff at Bell Northern Research, Ottawa, ON, Canada, where he did some of the early research in integrated, switched-capacitor networks. Between 1980 and 1992, he was consecutively an Assistant, Associate, and Full Professor at the University of California at Los Angeles. In 1991, he accepted the endowed Stanley Ho Professorship in Microelectronics at the University of Toronto. In 1998, he co-founded Snowbush Microelectronics along with Prof. David Johns where he is currently President while on a temporary leave of absence from the Univeristy of Toronto. He has authored or coauthored two textbooks entitled *Analog Integrated Circuit Design* (New York: Wiley, 1997) and *Digital Integrated Circuit Design* (New York: Oxford, 2000) in addition to three research books coauthored with former Ph.D. students. He has published well over 100 papers and holds five patents.

Dr. Martin was selected by the IEEE Circuits and Systems (CAS) Society for the Outstanding Young Engineer Award that was presented at the IEEE Centennial Keys to the Future Program in 1984. He was awarded a National Science Foundation Presidential Young Investigator Award (1985–1990) and the 1999 CAS Golden Jubilee Medal of the IEEE CAS Society. He was a co-recipient of the Beatrice Winner Award at the 1993 International Solid-State Circuits Conference and of the 1999 IEEE Darlington Best-Paper Award for the IEEE TRANSACTIONS ON CIRCUITS AND SYSTEMS. He was appointed as the IEEE CAS Press Representative (1985–1986). He was elected by the CAS Society members to their administrative committee (ADCOM 1985–1987), and as a member of the CAS Board of Governors (1995–1997). He served as an Associate Editor of the IEEE TRANSACTIONS ON CIRCUITS AND SYSTEMS from 1985 to 1987 and as an Associate Editor of PROCEEDINGS OF THE IEEE (1995–1997) and has served on the technical committee for many International Symposia on CAS and on the Analog Program Committee of the International Solid-State Circuits Committee. He gave an invited Plenary talk at the 2003 European Solid-State Circuits Conference (ESSCIRC).